



Full Quantum Simulation of Silicon-on-Insulator Single-Electron Devices

FREDERIK OLE HEINZ, ANDREAS SCHENK, ANDREAS SCHOLZE AND WOLFGANG FICHTNER
Integrated Systems Laboratory, ETH Zentrum, Gloriastrasse 35, CH-8092 Zürich, Switzerland

frederik.heinz@iis.ee.ethz.ch

Abstract. We present a method which extends the range of applicability of the domain decomposition approach to tunneling transport. Thereby we gain the ability to simulate e.g. structures with geometrically confined semiconductor quantum dots surrounded by very thin layers of dielectric or quantum dots that are defined through a combination of electrostatic forces and geometric confinement. Recently, experimental data of single electron devices on the 10 nm length-scale have become available, but due to the smallness of the devices detailed information on their geometry is hard to come by. Thus the simulations presented in this paper are intended as proof of principle rather than quantitative results for a real device. For predictive simulations more detailed knowledge of the experimental geometry is required.

Keywords: quantum dot, tunneling, domain decomposition, 3D, SOI, single electron transistor

1. Introduction

In the ongoing quest for ever smaller device dimensions and higher integration densities single electron devices might be able to play an important role. In this work we focus on silicon on insulator (SOI) single electron devices with direct tunneling as the dominant charge transport mechanism. The simulation geometry of an SOI single electron transistor (SET) is depicted in Fig. 1. It is derived from an experimental structure manufactured at the University of Tübingen (Augke *et al.* 2000). The diameter of the spherical quantum dot is 20 nm. The tunneling barriers reside in the constrictions in the silicon on either side of the central sphere.

2. Simulation Strategy

The quantum-mechanical charge density inside the device is computed by self-consistent solution of the Schrödinger–Poisson equations in effective mass approximation. In order to reduce the computational effort, the simulation volume is decomposed into domains of different dimensionality: source and drain contact regions are treated as two-dimensional electron gas; inside the quantum wires Schrödinger’s equation is

adiabatically decomposed into a 1D array of 2D equations. Only inside the quantum dot the solution of the full 3D eigenvalue problem is necessary.

From the self-consistent single-particle wavefunctions in the diverse regions we then may obtain tunneling rates by Bardeen’s transfer Hamiltonian method (cf. e.g. Payne (1986)). Subsequently we compute the linear response conductance of the device according to the approach by Beenakker (1991).

3. Adaptation of the Simulation Environment

The SIMNAD simulation environment (Scholze, Schenk and Fichtner 2000), developed at ETH, was originally designed for self-consistent conductance simulations of III–V single electron devices. In these devices quantum wires and dots were defined electrostatically by depletion of a 2DEG underneath metal electrodes. In contrast, SOI devices possess a fully three-dimensional geometry; electron localization is due to a combination of electrostatic forces and the geometrical confinement by the surrounding oxide. Also, in silicon we have to deal with a six-valley band structure with non-spherical iso-energy surfaces, whereas previously only spherical single-valley band structures

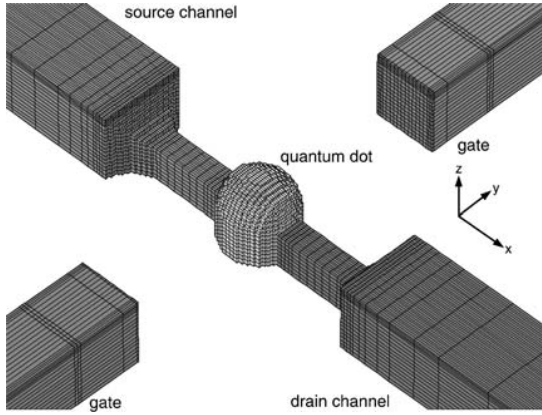


Figure 1. Simulation geometry of an SOI single electron transistor (oxide and substrate Si removed).

had to be considered. These differences necessitate several extensions to the simulation model.

3.1. Treatment of the Non-Spherical Six-Valley Band Structure of Silicon

In the effective mass approximation the six valleys of the silicon band-structure give rise to a Hamiltonian \mathcal{H}_{tot} operating on a Hilbert space of six component wave-functions. By neglecting inter-valley coupling, however, the full multi-valley Hamiltonian \mathcal{H}_{tot} may be decomposed into an (outer) direct sum of single-valley Hamiltonians

$$\mathcal{H}_{\text{tot}} \approx \bigoplus \mathcal{H}_{\alpha_i}, \quad (1)$$

$$\alpha \in \{x, y, z\}$$

$$i \in \{+, -\}$$

$$\mathcal{H}_{\alpha_{\pm}} = -\frac{\hbar^2}{2} \nabla \cdot \left(\left[\frac{1}{m_{\alpha}^*} \right] \nabla \right) - eV_s[\rho], \quad (2)$$

where $\left[\frac{1}{m_{\alpha}^*} \right]$ denotes the reciprocal effective mass tensor in a coordinate frame such that the main axis associated with its greatest mass component is along the α -axis, and $V_s[\rho]$ is the self-consistent potential brought about by ρ , the sum of the electron densities in all valleys. Thus the task of solving the 6-component Schrödinger equation is reduced to that of solving three scalar equations ($\mathcal{H}_{\alpha_+} = \mathcal{H}_{\alpha_-}$).

3.2. Handling of Moving Tunneling Barriers

In the SOI single electron transistor (SET) of Fig. 1 the definition of the quantum dot is due to a combination

of geometry and electrostatic effects. The variation of the transverse quantum kinetic energy along the transport direction is of the same order of magnitude as the depth of the electrostatic potential well inside the quantum dot region: depending on the gate voltage, a point may be found on either side of the tunneling barrier (cf. Fig. 2). Therefore, the simple strategy of defining a fixed Schrödinger box with Dirichlet boundary condition for the computation of the quantum dot levels breaks down: if the box is chosen too small, artificial boundary conditions will disturb the solution; if it is chosen too large, the Schrödinger solver will find solutions which are localized on the wrong side of the barrier (“spurious states”).

This may be remedied by modifying the Hamiltonian for the 3D Schrödinger box in the spirit of

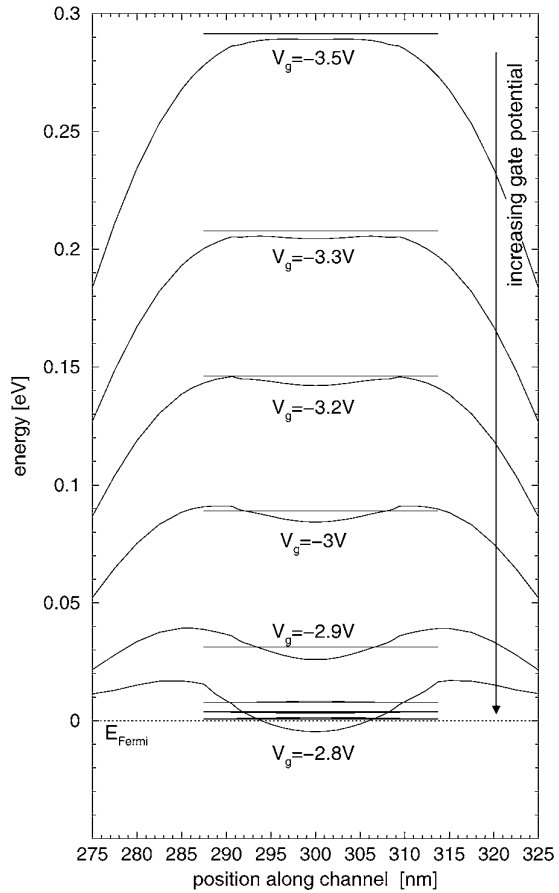


Figure 2. Quantum corrected conduction band energy and 3D eigen-energies at different gate voltages.

Bardeen's transfer Hamiltonian method: In 1D the transfer Hamiltonians $\mathcal{H}_{l/r}$ to either side of the barrier may be constructed by finding the position x_{\max} of the maximum of the barrier potential. The potential for $\mathcal{H}_{l/r}$ then is the unmodified potential $V(x)$ left/right of x_{\max} and $V(x_{\max})$ on the other side.

For higher dimensions this approach may be generalized by introducing the escape energy ϵ_{esc} : let x_0 be a point which is known to reside in the active dot volume (e.g. the minimum of the central potential well in the Schrödinger box). The escape energy then is the minimum energy at which there exists a classical trajectory from x_0 to infinity (i.e. to the boundary of the 3D Schrödinger domain, provided that it is chosen sufficiently large). Points x that may be reached classically from x_0 at energies smaller than ϵ_{esc} are said to be "inside" the *active* quantum dot volume Ω_{dot} . By leaving the potential inside Ω_{dot} unchanged and lifting it to at least ϵ_{esc} outside we may then construct a new Hamiltonian \mathcal{H}_{dot} (cf. Fig. 3).

This construction is often successful in eliminating the spurious states. But in some situations it is too crude: it is blind to pure geometrical confinement. This shortcoming may be overcome by means of a quantum-corrected effective potential

$$\tilde{V}(x) := V(x) + \max_{|\hat{v}|=1} \epsilon_{\text{trans}}(x, \hat{v}), \quad (3)$$

where the transverse kinetic energy $\epsilon_{\text{trans}}(x, \hat{v})$ is defined as the expectation value of the kinetic energy operator for the lowest 2D state in a plane through x at normals to \hat{v} . The maximum is taken such that inside a constriction the dominant direction is selected. This new potential \tilde{V} then is used to construct a modified escape energy $\tilde{\epsilon}_{\text{max}}$ and active dot volume $\tilde{\Omega}_{\text{dot}}$ as above.

The improved quantum dot transfer Hamiltonian $\tilde{\mathcal{H}}_{\text{dot}}$ then is defined as

$$\tilde{\mathcal{H}}_{\text{dot}} := -\frac{\hbar^2}{2} \nabla \left[\frac{1}{m^*} \right] \nabla + \begin{cases} V(x) : x \in \tilde{\Omega}_{\text{dot}} \text{ or } \tilde{V}(x) \geq \tilde{\epsilon}_{\text{esc}} \\ \tilde{\epsilon}_{\text{esc}} - \epsilon_{\text{trans}}(x) : \text{otherwise} \end{cases} \quad (4)$$

The same method may also be used for quantum dots that are separated from neighboring semiconductor regions by a very thin layer of dielectric: here the Schrödinger box must extend some distance into the semiconductor on the other side of the dielectric such that the wave-function can recover from the Dirichlet

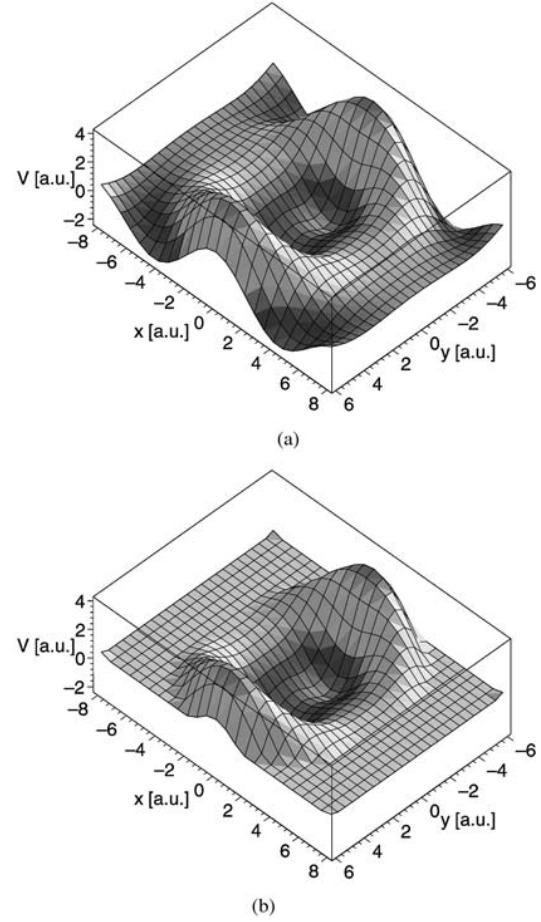


Figure 3. Example potential (a) unmodified (b) modified.

condition imposed on the box boundary; this will again bring about spurious states, that can be eliminated by the above method.

4. Results

With the modified transfer Hamiltonian $\tilde{\mathcal{H}}_{\text{dot}}$ the occurrence of spurious wave-functions could indeed be suppressed: all bound states are localized within the active dot volume, and there is almost no deformation due to the modified potential (cf. Fig. 4); the eigenenergies of the allowable single particle eigenstates were changed by less than $10 \mu\text{eV}$ (the numerical precision of the simulator).

The effective mass anisotropy has a pronounced effect on the shape of the wave-functions: depending

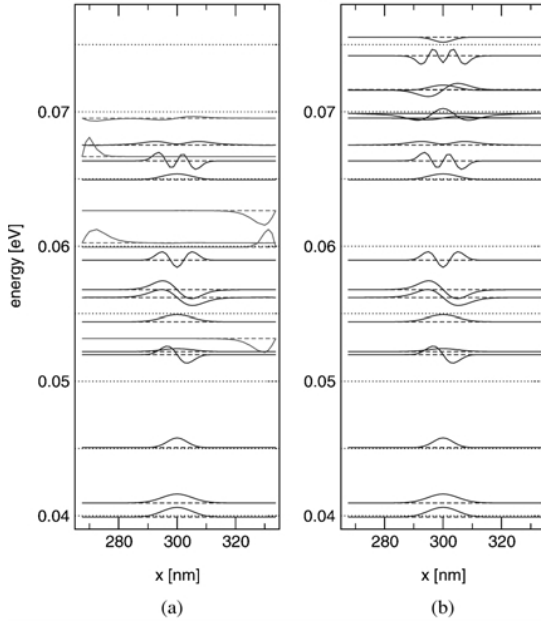


Figure 4. One-dimensional cuts through the eigenstates of (a) the original Hamiltonian \mathcal{H} ; (b) the improved transfer Hamiltonian $\tilde{\mathcal{H}}_{\text{dot}}$ [note the suppression of the spurious states by $\tilde{\mathcal{H}}_{\text{dot}}$].

on the orientation of the reciprocal effective mass tensor their spread along the transport direction varies so strongly that the tunneling rates of corresponding states in different valleys diverge by up to 8 orders of magnitude (cf. Fig. 5). The strong suppression of tunneling for $n_y = 2$ states relative e.g. to $n_z = 2$ states (where applicable the wave-functions are labelled by particle-in-a-box quantum numbers $n_x n_y n_z$) results from the symmetry of the structure in y -direction (the maximum of the channel wave-function coincides with a node of the dot wave-function) as opposed to the off-center position of the channel in z -direction: the quantum wire enters the quantum dot in the cylindrical bottom section, but is centered along the y -axis (cf. Fig. 1). The straight lines joining series of states (e.g. 111-211-311-411-511 for the $m_{\text{max}}^* = m_x^*$ orientation) correspond to an exponential increase of Γ with single particle energy.

The onset of conduction was found near a gate voltage of -2.5 V. Given that the simulation was modeled on a low resolution micrograph of the experimental structure together with the text description in Augke *et al.* (2000) this is in reasonable agreement with the experiment (experiment: first peak near -2.9 V). We find

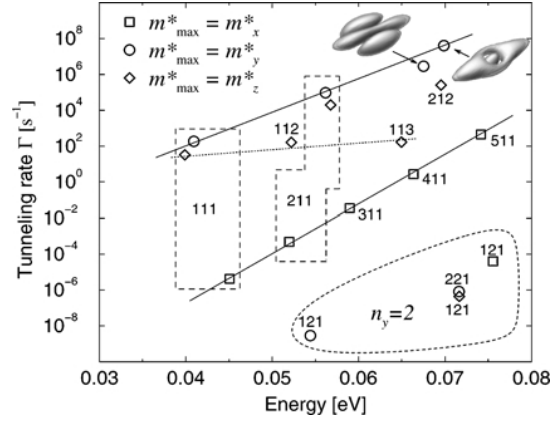


Figure 5. Source-dot tunneling rates of the single particle wave-functions (particle-in-a-box quantum numbers $n_x n_y n_z$ shown where appropriate).

a spacing of the conductance peaks of about 100 mV, which also is not too far off from the experimental data.

5. Conclusions

In this paper we have been mostly concerned with technical difficulties that arise in the self-consistent quantum-mechanical simulation of SOI single electron devices. Now that they are overcome more detailed information on the device geometry is necessary in order to give true predictive power to our simulator. Only then will it be possible to decide the crucial question of whether a proposed device operates according to controllable conditions such as geometrical structure, or whether it depends on uncontrollable conditions such as an opportune configuration of individual dopant atoms, thus making reproducible production of such devices infeasible.

Acknowledgment

This work was funded by the European Union under contract number IST-1999-10828 (NANOTCAD).

References

- Augke R., Eberhardt C., Single F., Prins F.E., Wharam D.A., and Kern D.P. 2000. Appl. Phys. Lett. 76(15): 2065.
- Beenakker C.W.J. 1991. Phys. Rev. B 44: 1646.
- Payne M.C. 1986. The Institute of Physics, pp. 1145–1154.
- Scholze A., Schenk A., and Fichtner W. 2000. IEEE Trans. Elec. Dev. 47(10): 1811.